JOURNAL OF AGRICULTURAL AND FOOD CHEMISTRY

Article

pubs.acs.org/JAFC

# Nanocomposite PAAm/Methyl Cellulose/Montmorillonite Hydrogel: Evidence of Synergistic Effects for the Slow Release of Fertilizers

Adriel Bortolin,[†,‡] Fauze A. Aouada,[§] Luiz H. C. Mattoso,[‡] and Caue Ribeiro*[,‡]

[†]Departamento de Química, Universidade Federal de São Carlos, 13565-905, São Carlos, SP, Brazil

[‡]Laboratório Nacional de Nanotecnologia aplicado ao Agronegócio (LNNA)-Embrapa Instrumentação (CNPDIA), 13560-970, São Carlos, SP, Brazil

[§]Departamento de Física e Química, Faculdade de Engenharia de Ilha Solteira, Universidade Estadual Paulista-UNESP, 15385-000 Ilha Solteira, SP, Brazil

*S* *Supporting Information*

**ABSTRACT:** In this work, we synthesized a novel series of hydrogels composed of polyacrylamide (PAAm), methylcellulose (MC), and calcic montmorillonite (MMt) appropriate for the controlled release of fertilizers, where the components presented a synergistic effect, giving very high fertilizer loading in their structure. The synthesized hydrogel was characterized in relation to morphological, hydrophilic, spectroscopic, structural, thermal, and kinetic properties. After those characterizations, the application potential was verified through sorption and desorption studies of a nitrogenated fertilizer, urea ($CO(NH_2)_2$). The swelling degree results showed that the clay loading considerably reduces the water absorption capability; however, the hydrolysis process favored the urea adsorption in the hydrogel nanocomposites, increasing the load content according to the increase of the clay mass. The FTIR spectra indicated that there was incorporation of the clay with the polymeric matrix of the hydrogel and that incorporation increased the water absorption speed (indicated by the kinetic constant $k$). By an X-ray diffraction technique, good nanodispersion (intercalation) and exfoliation of the clay platelets in the hydrogel matrix were observed. Furthermore, the presence of the montmorillonite in the hydrogel caused the system to liberate the nutrient in a more controlled manner than that with the neat hydrogel in different pH ranges. In conclusion, excellent results were obtained for the controlled desorption of urea, highlighting the hydrolyzed hydrogels containing 50% calcic montmorillonite. This system presented the best desorption results, releasing larger amounts of nutrient and almost 200 times slower than pure urea, i.e., without hydrogel. The total values of nutrients present in the system show that this material is potentially viable for application in agriculture as a nutrient carrier vehicle.

**KEYWORDS:** *hydrogel nanocomposites, polyacrylamide, montmorillonite clay, hydrolysis process, controlled release of fertilizer*

## INTRODUCTION

Nitrogen is one of the essential elements for good soil fertility, and among the available commercial options for its application, one of the most economically viable is the urea, $CO(NH_2)_2$. However, this compound is not very efficient as a fertilizer.[1] The loss of nitrogen to the atmosphere via volatilization of ammonia is one of the main factors responsible for the low efficiency of urea applied on the soil surface. The amount of nitrogen lost through volatilization, after soil surface application of urea, can reach extreme values close to 80%.[2] That justifies the great interest in developing alternatives that allow slow nitrogen liberation in the soil and consequent better administration.

To overcome such problems, hydrogels have emerged as a good alternative. Hydrogels are extremely hydrophilic polymers that have the characteristic of absorbing large amounts of water, as an agricultural input, and make it available to the plants over a long period. Hydrogels based on polysaccharides[3] are receiving great attention in the agriculture sector because they are immediately related to soil water retention, when used as conditioners. Their formulation from polysaccharides ensures greater improvements in biodegradability and slow release properties of materials.[4−6] The main benefit of the controlled release system is to increase the functional efficiency of a certain input, reducing costs, as well as increasing the product handling safety, reducing toxicity risks for humans due to high concentrations in the field, and reducing environmental contamination[7] with the objective of maintaining the concentration of the input in a range considered optimum for an extended time starting from a single application.

However, in spite of the benefits for the use of the hydrogel, the final price of the product in the market ends up making its application unfeasible. To solve that problem, one of the alternatives is to form a nanocomposite from hydrogels with clay minerals[8−10] in high proportions, which reduces the final value of the product drastically and still improves some very important properties, such as ion exchange capacity,[11,12] water absorption speed, and mechanical resistance.[13,14] The viability for hydrogel use is enhanced even more by the hydrolysis treatment of the material because such treatment improves its hydrophilic properties considerably.[15]

**Received:** March 26, 2013
**Revised:** July 1, 2013
**Accepted:** July 3, 2013
**Published:** July 3, 2013

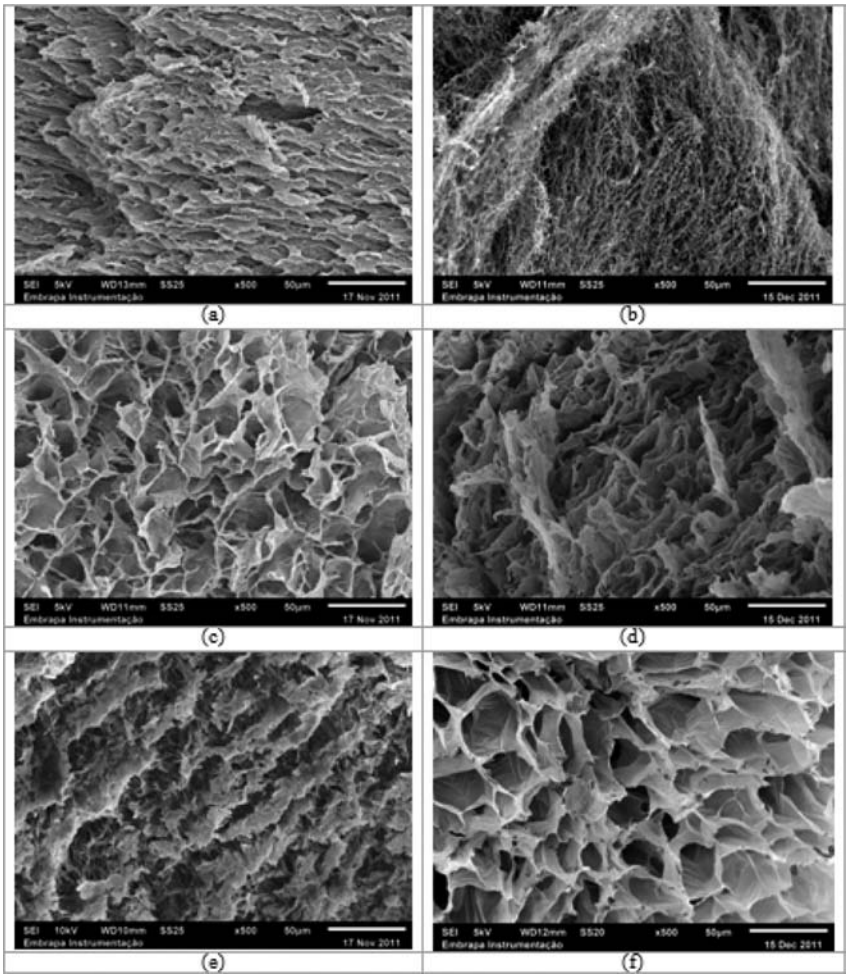

**Figure 1.** SEM micrographs for (a) (1:0) neat hydrogel; (b) (1:0) hydrolyzed neat hydrogels; (c) (1:1) hydrogel; (d) (1:1) hydrolyzed hydrogel; (e) (3:1) hydrogel; (f) (3:1) hydrolyzed hydrogel.

As such this, in this work, we conducted the synthesis of a new hydrogel nanocomposite, composed of polyacrylamide (PAAm), using the biodegradable polysaccharide methylcellulose (MC) and the clay mineral calcic montmorillonite (MMt) as modifiers. Such materials were characterized regarding their hydrophilic, spectroscopic, kinetic, structural, mechanical, morphological, and thermal properties, and the controlled desorption of the nutrient urea.

## MATERIALS AND METHODS

**Synthesis of Nanostructured Hydrogels.** The hydrogels composed of polyacrylamide (PAAm) and the biodegradable polysaccharide methylcellulose (MC; molar mass, 40.000 g $mol^{-1}$; viscosity, 400 cP; 27.5−31.5% methyl groups; and 68.5−72.4% hydroxyl groups; data supplied by the manufacturer Aldrich) and calcic montmorillonite (MMt) were obtained through chemical polymerization of the acrylamide monomer (AAm, Fluka) in aqueous solution containing MC and MMt. The AAm, MC, and *N*,*N*,*N*′,*N*′-tetramethylethylenodyamine catalyzer (TEMED, Sigma) concentrations were kept constant at 3.73 wt %, 0.50 wt %, and 3.21 $\mu$mol.$mL^{-1}$, respectively. The concentration of the *N*′-*N*-methylene bisacrylamide (MBAAm, Aldrich) cross-linking agent was fixed at 2.30 mol % relative to the AAm concentration. The MMT concentration was varied regarding the mass of AAm + MC used in the synthesis. The synthesis of hydrogels was started by a first solubilization of AAm in water followed by a dispersion of MMT into AAm solution. The cross-linking agent MBAAm and TEMED were added, and they were mechanically stirred during 30 min. After preparing the mixture, $N_2$ was bubbled into the solution for 20 min to remove oxygen. Finally, sodium persulphate ($Na_2S_2O_8$, Sigma) (3.38 $\mu$mol.$mL^{-1}$) was added in order to initiate the polymerization reaction by the free radical mechanism. After this process, the hydrogel was purified by immersion in water during 4 days. The hydrogels were then named as hydrogel 1 (1:1 or 50% hydrogel: 50% MMt in weight); hydrogel 2 (2:1 or 66% hydrogel: 33% MMt); hydrogel 3 (3:1 or 75% hydrogel: 25% MMt); hydrogel 4 (4:1 or 80% hydrogel: 20% MMt); and hydrogel 5 (1:0 or neat hydrogel).

**Physicochemical Characterization of Nanostructured Hydrogels.** *Swelling Degree.* The hydrophilicity of the hydrogels was investigated through swelling degree measurements (Q). The swelling degree can be calculated as the ratio between the mass of the swollen hydrogel and the mass of the dry hydrogel.[16,17] The hydrogels were placed directly in contact with Milli-Q water and/or urea solution, and the swelling degree values were monitored at predetermined times, thus being able to accompany its swelling kinetics.

*Swelling Degree after the Hydrolysis Process.* The dry cylindrical-shaped hydrogels were placed in a 0.5 mol $L^{-1}$ NaOH solution and left to swell during 18 h at 75 °C. These conditions were achieved after initial investigation by variation of temperature and hydrolysis time parameters. The hydrolyzed hydrogels were put in Milli-Q water, and the swelling degree was monitored for 24 h.

*Fourier Transform Infrared Spectroscopy (FTIR).* The spectroscopic characterization of the hydrogel nanocomposites was conducted through Fourier transform infrared spectroscopy (FTIR) using a spectrometer (Perkin-Elmer Spectrum, Paragon 1000 model). The synthesized hydrogels were dried, mixed with potassium bromide (KBr), and pressed forming (KBr) tablets.[18,19] FTIR spectra were

obtained registering 128 scans from 400 to 4000 $cm^{-1}$, with a resolution of 2 $cm^{-1}$.

*X-ray Diffraction.* The structural properties of clay samples in powder form and the PAAm-MC hydrogels and hydrogel nanocomposites containing different clay contents were analyzed using the X-ray diffraction technique. A Shimadzu LabX XDR-6000 diffractometer was used, operating with an emission tube acceleration voltage of 30 kV, current of 30 mA, and Cu $K_\infty$ ($\lambda$ = 0.154 nm) radiation. The scanning velocity used was 1.0° $min^{-1}$ and the Bragg angle reading between 3° and 60°.

*Scanning Electron Microscopy (SEM).* After being swollen until equilibrium in water, the hydrogels were removed and immersed in liquid nitrogen. Later, the samples were lyophilized (freeze-dried) for 48 h. After lyophilization, the hydrogels were placed in a sample holder and their surfaces covered with a gold thin layer.[20,21] Such a procedure was adopted to avoid the collapse of the hydrogel porous structure, thus guaranteeing that all of the morphological characteristics obtained for the dry hydrogels can be used for the hydrogels in the swollen state.[22] The micrographs of the hydrogels were obtained using a scanning electronic microscope JEOL (Model JSM-6510).

*Kinetic Parameters.* The swelling kinetics parameters were obtained through kinetic measures of $Q$ for the different synthesized hydrogels. For each curve, the difusional exponent ($n$) and diffusion constant ($k$) were calculated using eq 1:[23]

$$\frac{M_t}{M_{eq}} = kt^n \quad (1)$$

where $t$ is the time, $k$ is the diffusion constant and depends on the type of hydrogel and the swelling medium, and $n$ is the diffusional exponent, which supplies information on the type of transport mechanism that impels the sorption of a given solute. $M_t$ and $M_{eq}$ are the masses of the hydrogel at a swelling time "$t$" and in the equilibrium state, respectively.

The equation can be applied from the initial stages until approximately 60% because at that stage, the increase of the swelling degree over time is an ascending straight line. After that period, as the swelling tends toward equilibrium, that is, it practically does not undergo more variation over time, the inclination of the straight line is practically null (tangent ≈ 0). For the calculation of $n$ and $k$, ln $M_t/M_{eq}$ vs ln $t$ graphs were made for each assay, and the difusional coefficient $n$ was obtained from the angular coefficient and $k$ from the linear coefficient.

*Sorption and Desorption of Urea in Water.* Since one of the main objectives of this work was to observe how the hydrogel behaves in the controlled desorption of a fertilizer, a kinetic test was carried out in aqueous medium. This study had the objective of determining the release in water of the fertilizing compound, contained in the hydrogel after 72 h of being submerged in a saturated solution of urea. The model used was adapted from that proposed by Jijun et al.[24] for the evaluation of the slow release of drugs. Following that model, an apparatus was set up here, where the hydrogels swollen in saturated solution of urea were placed in a submerged small beaker in aqueous medium, at pH 7.0, under magnetic stirring external to the beaker containing the hydrogel. This procedure guaranteed that the urea content measured in the liquid medium corresponded to the diffusion into the medium and not to the mechanical action of the stirrer. Aliquots were collected at different pre-established time intervals, until the limit of 196 h. Desorption measurements were conducted in triplicate. For comparison, a test was also conducted with pure urea as experimental control, where an amount of urea intermediate to that present in the hydrogels was stipulated.

The determination of the urea concentration in solution was done by analysis in a UV−vis spectrophotometer, according to methodology proposed by With et al.[25] The methodology consists of preparing the Ehrlich reagent (5g of dimethylaminobenzaldehyde + 20 mL of concentrated hydrochloric acid, to complete 100 mL) and 10% solution trichloroacetic acid. To take the reading in the UV−vis spectrophotometer, 0.5 mL of the sample to be analyzed was mixed with 2.0 mL of the acid solution and 0.5 mL of the Ehrlich reagent (in the described sequence). From that, a curve of the nitrogen concentration in solution versus absorbance in the $\lambda$ = 420 nm region (calibration curve) can be obtained, and through that, the urea desorption values as a function of time starting from the hydrogels can be arrived at.

The desorption was analyzed using the model proposed by Reis et al,[32] where the fractional release ($F_R$) was estimated assuming the total urea loading as proportional to the maximum swelling degree. This value was plotted against time assuming first and second order equilibrium release kinetics, observing the $R^2$ values for each proposition. The value $\alpha = F_{MAX}/(1 - F_{MAX})$ was calculated for all of the conditions analyzed, using this value to estimate the affinity of the solute for the nanocomposite hydrogel or for the solvent (water).

## RESULTS AND DISCUSSION

**Physical Characterization.** The morphological investigation of the hydrogels composed of PAAm-MC and calcic montmorillonite (MMt) was conducted by scanning electronic microscopy, as seen in Figure 1. The morphologies of those hydrogels presented quite homogeneous foliaceous structures, which are characteristics of hydrogels composed of polysaccharides.[26] The hydrogels without the hydrolysis treatment did not present significant changes in pore morphology with the addition of the clay (Figures 1a, c, and e). However, after the hydrolysis treatment, two different behaviors can be observed: (i) general increase in pore size due to the higher swelling degree; (ii)

**Table 1. Quantitative Analysis of the Evidence Presented in the EDX Map of the Hydrogel with 50% MMt**

| element | weight percent | atomic percent |
|---|---|---|
| C | 2.22 | 3.73 |
| N | 7.60 | 10.96 |
| O | 37.19 | 47.00 |
| Na | 0.67 | 0.59 |
| Mg | 2.14 | 1.78 |
| Al | 13.27 | 9.95 |
| Si | 34.43 | 24.79 |
| K | 0.80 | 0.42 |
| Ca | 0.86 | 0.43 |
| Ti | 0.83 | 0.35 |
| **Total** | **100** | **100** |

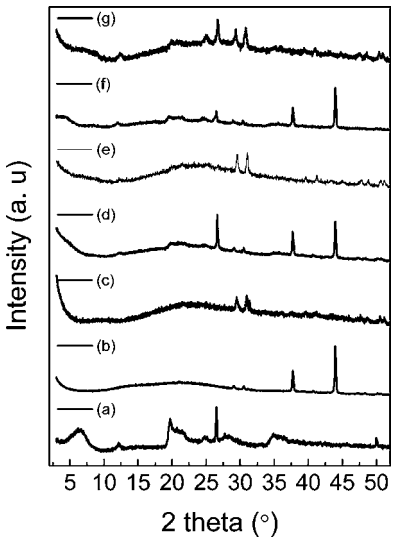


**Figure 2.** X-ray diffraction (XRD) patterns of the (a) MMT clay; (b) (1:0) neat hydrogel; (c) (1:0) hydrolyzed neat hydrogel; (d) (3:1) hydrogel; (e) (3:1) hydrolyzed hydrogel; (f) (1:1) hydrogel; and (g) (1:1) hydrolyzed hydrogel.


dx.doi.org/10.1021/jf401273n | J. Agric. Food Chem. 2013, 61, 7431−7439

**Table 2. FTIR Band Characteristics of Hydrogels Synthesized**

| materials | spectroscopic attributions |
|---|---|
| PAAm | |
| 3300−3450 $cm^{-1}$ | stretching vibration of $NH_2$ |
| 1667 and 1466 $cm^{-1}$ | axial deformation of C═O |
| MC | |
| 2990−3600 $cm^{-1}$ | stretching vibration of OH. |
| 900−1230 $cm^{-1}$ | $\beta$-glycosides bonds among saccharide units |
| 620 $cm^{-1}$ | band attributed to pyronisidic ring |
| calcic montmorilonite | |
| 400 − 800 $cm^{-1}$ | Si-O-M bending vibrations |
| 914−930 $cm^{-1}$ | Al-OH-Al angular vibrations |
| 1010−1110 $cm^{-1}$ | symmetric stretching of Si−O |
| 3620−3630 $cm^{-1}$ | axial deformation of structural −OH |

decrease in pore sizes with the addition of clay mineral, indicating that the load affected the crossing of the chain in the formation of the hydrogel.

The dispersion of the clay in the hydrogel matrix was observed by energy dispersive spectrometry X-ray measurements (EDX). Table 1 displays the semiquantitative analysis of the respective elements present in the EDX map. The presence of all of the elements that constitutes the calcic montmorillonite clay mineral (structural formula: $Ca_{0.6}(Al,Mg)_2Si_4O_{10}(OH)_2{\cdot}nH_2O$) may be observed, indicating its effective incorporation. The mapping of Si and Al elements, coming exclusively from the clay mineral in those nanocomposites, indicates that good clay dispersion occurred in the polymeric matrix, by comparison with the dispersion of the element C, indicative of the hydrogel (Supporting Information, Figure 1).

Figure 2 presents the X-ray diffractograms of MMt, PAAm, and MC hydrogel and its nanocomposites prepared with different clay contents with and without hydrolysis treatment. The interlamelar spacing or basal interplanar spacing ($d_{001}$) of the samples was calculated from the respective diffraction peaks using Bragg's law, eq 2:

$$n\lambda = 2d_{001} \sin\theta \quad (2)$$

where $\theta$ = incidence angle; $n$ = reflection order; and $\lambda$ = incident radiation wavelength ($\lambda$ = 0.154 nm).

The X-ray diffractogram of the pure clay showed an intense peak at 2 $\theta$ = 6.56°, referring to the basal plane and corresponding to the interlamelar distance $d_{001}$ = 1.35 nm, which identifies the montmorillonite phase, as expected. Peaks at 25 and 27° are also observed, corresponding to possible quartz contamination, commonly present in materials of mineral origin.[27,28] Diffraction peaks at 28, 31, 38, and 45° are observed

**Table 3. Values of Parameters *n* and *k* for Hydrogels Synthesized**

| hydrogel | $k$ ($h^{-1}$) | $n$ |
|---|---|---|
| 1 | 0.27 ± 0.04 | 0.63 ± 0.02 |
| 2 | 0.22 ± 0.01 | 0.57 ± 0.02 |
| 3 | 0.19 ± 0.01 | 0.64 ± 0.02 |
| 4 | 0.18 ± 0.01 | 0.65 ± 0.03 |
| 5 | 0.17 ± 0.01 | 0.49 ± 0.02 |

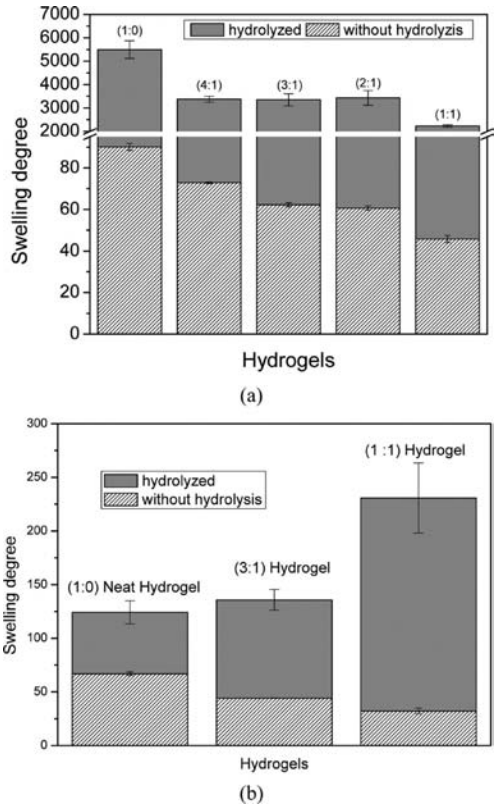


**Figure 4.** Swelling degree at equilibrium for hydrogel samples with and without hydrolysis processes in (a) milli Q water and (b) urea saturated solution.

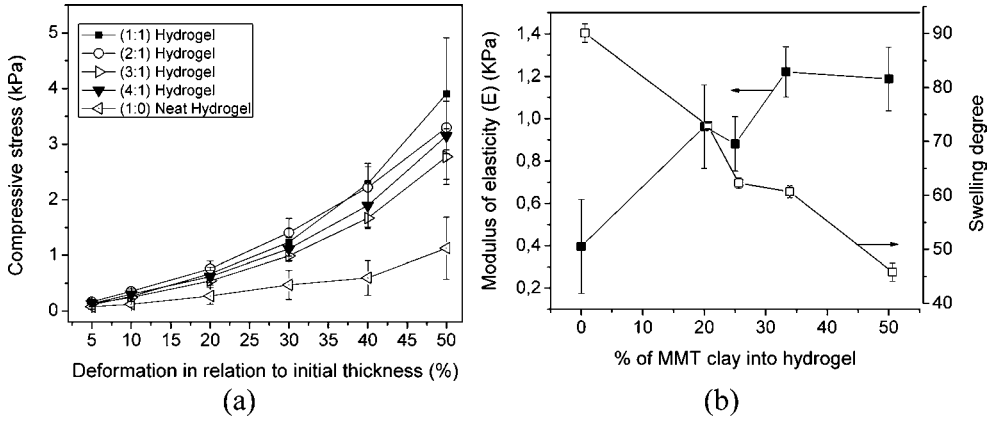


**Figure 3.** (a) Representative curves of stress-deformation for different hydrogels and (b) dependence of modulus of elasticity as a function of % of MMT clay into hydrogels.


dx.doi.org/10.1021/jf401273n | J. Agric. Food Chem. 2013, 61, 7431−7439

**Table 4. Swelling Degree at Equilibrium ($Q_{eq}$) before and after the Hydrolysis Process**

| hydrogel | $Q_{eq}$ (g/g) | $Q_{eq}$ hydrolyzed (g/g) | $Q_{eq}$ [a] (g/g) | $Q_{eq}$ hydrolyzed[a] (g/g) |
|---|---|---|---|---|
| 1 | 45.8 ± 1.7 | 2188.1 ± 53.4 | 32.1 ± 2.7 | 230.8 ± 32.7 |
| 2 | 60.7 ± 1.1 | 3241.4 ± 150.2 | 41.9 ± 0.1 | [b] |
| 3 | 62.3 ± 1.0 | 3382.5 ± 172.5 | 44.2 ± 0.2 | 135.7 ± 9.6 |
| 4 | 72.9 ± 0.5 | 3300.3 ± 128.0 | 47.1 ± 2.7 | [b] |
| 5 | 90.1 ± 1.7 | 5403.6 ± 378.9 | 66.9 ± 1.7 | 124.2 ± 10.8 |

[a]Swelling in saturated urea. [b]Not done in such conditions.

for the neat hydrogel, corresponding to the interplanar distances 3.18, 2.88, 2.63, and 2.09 Å. In the nanocomposite materials, peaks characteristic of clay were not observed in the region $2\theta$ = 3−10°, indicating good nanodispersion (intercalation) and exfoliation of the clay lamellae in the hydrogel matrix for all of the conditions, except the (1:1) condition, where the basal plane moved to 3.90°, which corresponds to $d_{001}$ = 2.26 nm. This behavior was expected because at this higher clay content, there is less quantity of hydrogel for lamellae separation. However, the displacement of the basal plane, even in this condition, indicates the good interaction of the clay mineral with the hydrogel. However, it was observed that the hydrolysis process facilitated the clay nanodispersion and exfoliation in the hydrogel matrix, allowing, in this condition, the disappearance of the basal plane. As will be discussed later, the more homogeneous distribution of the clay in the polymeric matrix will directly influence the water absorption capacity, urea fertilizer sorption/desorption time, and level of that same fertilizer starting from the studied nanocomposites. It is important to emphasize that the diffraction patterns were obtained in the dry materials, and therefore, the observed dispersion refers exclusively to the intercalation of the polymer in the lamellar structure of the clay and not to its swelling capacity.

**Table 5. Amount of Urea Desorbed (g of Urea/g of Dry Hydrogel) at Equilibrium for Unhydrolyzed Hydrogels at Differents pHs**

| hydrogel | pH 4 | pH 7 | pH 9 |
|---|---|---|---|
| 1 | 13.5 ± 1.0 | 10.2 ± 0.3 | 12.5 ± 0.3 |
| 3 | 19.4 ± 0.9 | 15.8 ± 0.7 | 20.9 ± 0.6 |
| 5 | 23.2 ± 0.2 | 15.1 ± 0.7 | 24.0 ± 1.9 |

Furthermore, the hydrolysis process is revealed in the diffractograms by the disappearance of the reflections regarding the interplanar distance of 2.63 and 2.09 Å, indicating that the base attack broke the rigid structure along the chains, probably reducing their average length. However, this effect probably does not alter the interaction among chains, probably associated with hydrogen bonds and revealed by the identification of the reflections at 3.18 and 2.88 Å. This is also indicative that this periodicity was maintained, even after the hydrolysis.

Table 2 displays the characteristic peaks identified by FTIR spectroscopy for the synthesized hydrogels (Supporting Information, Figure 2).

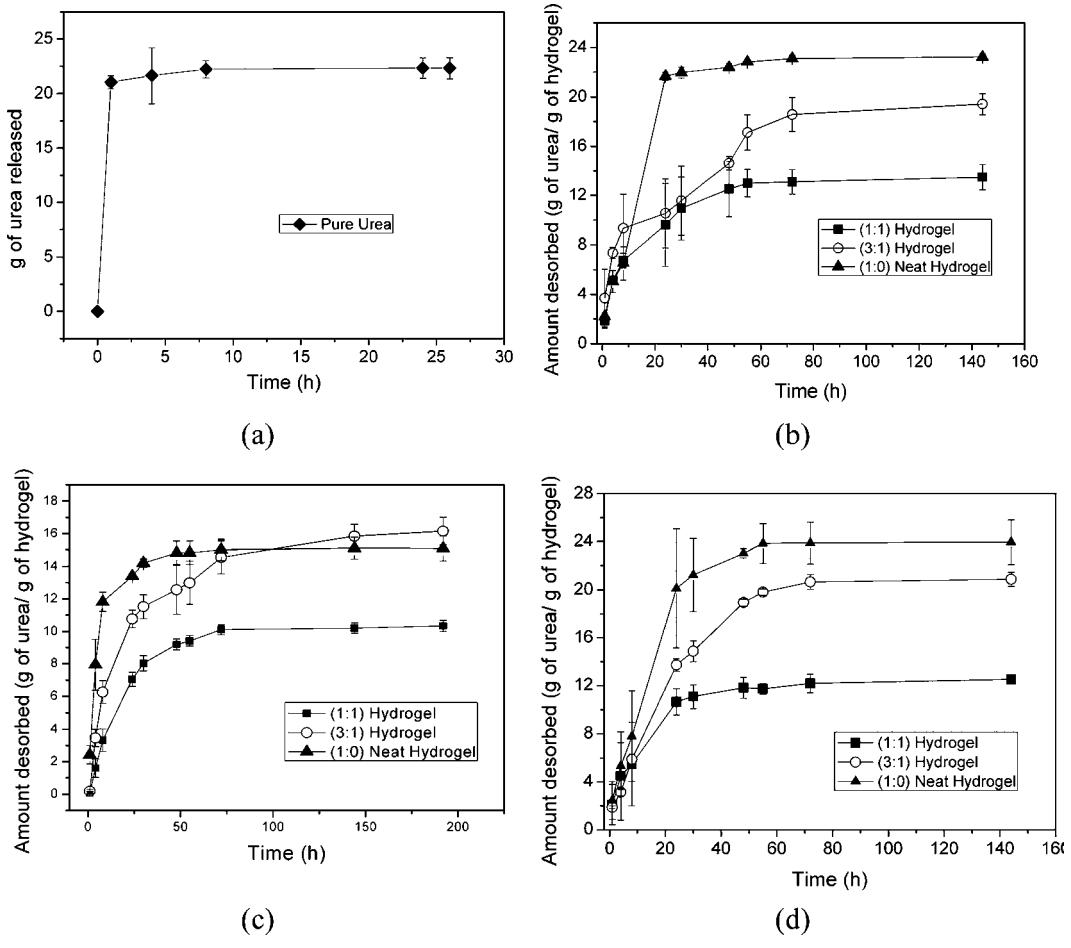


**Figure 5.** Kinetic curves of controlled desorption of urea for (a) pure spherical urea, and different hydrogels at (b) pH 4.0, (c) pH 7.0, and (d) pH 9.0.


dx.doi.org/10.1021/jf401273n | J. Agric. Food Chem. 2013, 61, 7431−7439

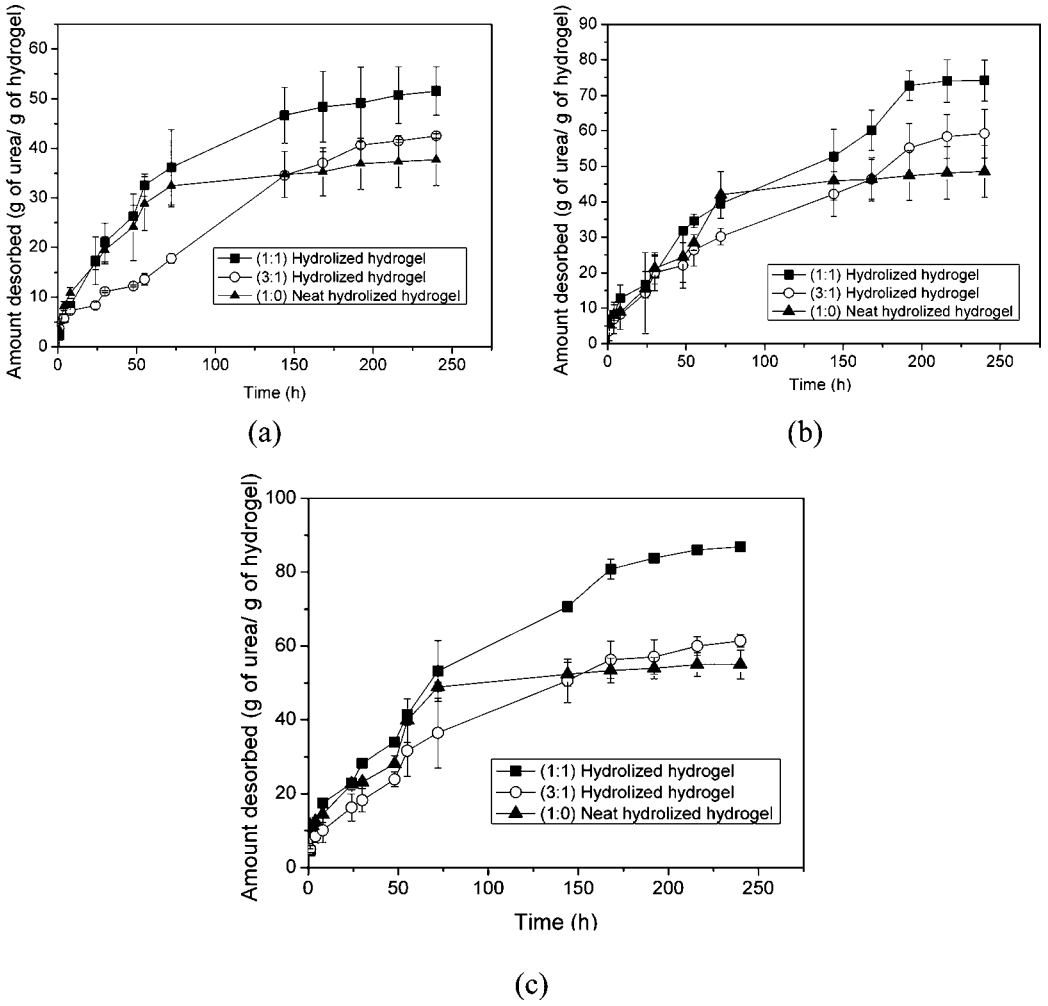


**Figure 6.** Kinetic curves of the controlled desorption of urea in different pH values for the hydrolyzed hydrogels: (a) 4.0; (b) 7.0; and (c) 9.0.

**Table 6. Amount of Urea Desorbed (g of Urea/g of Dry Hydrogel) at Equilibrium for Hydrolyzed Hydrogels at Differents pHs**

| hydrogel | pH 4 | pH 7 | pH 9 |
|---|---|---|---|
| 1 | 51.5 ± 4.8 | 74.2 ± 5.6 | 86.9 ± 1.0 |
| 3 | 45.0 ± 0.6 | 59.2 ± 6.8 | 61.4 ± 1.8 |
| 5 | 37.7 ± 5.2 | 48.5 ± 7.3 | 55.0 ± 4.0 |

For hydrogel 1, composed of PAAm-MC-MMt, all of the mentioned bands can be observed, indicating the effective incorporation of clay in the hydrogel. However, suppression or displacement of the hydrogel or clay bands was not observed, which indicates that the interlacing among the components is weak. It should be emphasized that the bonding between the hydrogel and the clay mineral lamellae ought to occur by ionic bonds between the hydrophilic groups of each material, which cannot be evidenced in FTIR. However, for the hydrolyzed

**Table 7. $\alpha$ and $R^2$ Values Obtained Using the Reis et al.[32] Model for Different Hydrogels Synthesized**

| | | hydrogels | | | hydrolyzed hydrogels | | |
|---|---|---|---|---|---|---|---|
| hydrogel | pH | $\alpha$ | $R^2$ (reversible first order kinetics) | $R^2$ (reversible second order kinetics) | $\alpha$ | $R^2$ (reversible first order kinetics) | $R^2$ (reversible second order kinetics) |
| (1:1) | 4.0 | 4.258 | 0.97663 | 0.97699 | 0.998 | 0.99800 | 0.99801 |
| | 7.0 | 1.577 | 0.94531 | 0.94477 | 2.556 | 0.98445 | 0.98413 |
| | 9.0 | 3.027 | 0.94562 | 0.94593 | 5.327 | 0.94951 | 0.97399 |
| (3:1) | 4.0 | 5.508 | 0,89262 | 0.88573 | 8.469 | 0.91772 | 0.91249 |
| | 7.0 | 2.226 | 0.9584 | 0.96425 | [a] | 0.99336 | 0.86601[b] |
| | 9.0 | 10.022 | 0.96517 | 0.95756 | [a] | 0.97193 | 0.78833[b] |
| (1:0) | 4.0 | 2.024 | 0.93838 | 0.93777 | [a] | 0.95296 | 0.94852[b] |
| | 7.0 | 0.770 | 0.96025 | 0.96011 | [a] | 0.95008 | 0.62798[b] |
| | 9.0 | 2.222 | 0.95511 | 0.95508 | [a] | 0.95233 | 0.42999[b] |

[a]The value was not calculated since $F_{max}$ tended to 1. [b]Calculated assuming alpha as constant (arbitrary).


dx.doi.org/10.1021/jf401273n | J. Agric. Food Chem. 2013, 61, 7431−7439

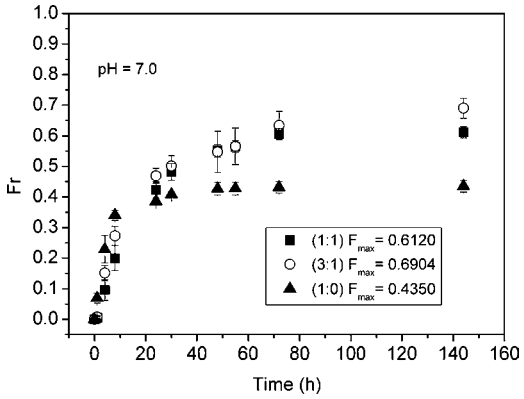


**Figure 7.** Fractional release ($F_r$) of urea from a nonhydrolyzed hydrogel at pH 7.0.

hydrogels, some changes are observed, mainly due to partial conversion of the amide groups to carboxylic groups, indicating the occurrence of a PAAm hydrolysis reaction. In a general way, the spectra for the hydrolyzed hydrogels were quite similar to the spectra of the hydrogels without hydrolysis. However, for the hydrolyzed hydrogels two bands were observed regarding the carboxylate ion ($-COO^-$), a more intense one in the region of 1630−1610 $cm^{-1}$ originating from the axial asymmetric deformation and another weaker one, observed around 1400 $cm^{-1}$ that stems from the axial symmetric deformation.[29] All of the hydrogels presented very defined peaks in the 1670 $cm^{-1}$ region, regarding the carbonyl stretching vibration in the acrylamide groups ($-CONH_2$), showing that the conversion of the amide groups into carboxylic groups is not complete in the alkaline hydrolysis reaction for the hydrogels. Usually, the conversion degree of the amide groups into carboxylic groups is below 70% under alkaline conditions.[30]

The evaluation of the mechanical properties of the hydrogels made up of PAAm, MC, and calcic montmorillonite was conducted determining the values of maximum compressive stress ($\sigma_{max}$) and modulus of elasticity ($E$) for different clay mineral contents present in the hydrogel. Representative force−deformation curves for different hydrogels using uniaxial deformation are shown in Figure 3, where good linearity is observed among the properties. This indicates that the deformation of the hydrogel is elastic, in other words, the hydrogel tends to return to its initial shape when the force applied to it is removed. It can also be observed that the increase in calcic montmorillonite concentration reduces the elastic region of the mechanical properties. Also observed is that the presence of the calcic montmorillonite provokes a considerable gain in mechanical resistance, requiring tension 4 times higher (hydrogel 1) so that it causes the same deformation as that in hydrogel 5 (1:0, i.e., without clay addition). As previously discussed, the increase of clay content in the polymeric matrix provokes a reduction of the swelling values. Figure 3b shows that the higher the hydrogel swelling degree, the lower its modulus tends to be; in other words, the higher the concentration of clay mineral in the polymeric matrix, the more resistant the hydrogel will be.

However, the hydrolysis process compromised the mechanical resistance of all of the samples, in spite of the sample with higher clay content presenting better manipulability, indicating that the reinforcement effect provided by the nanoload is maintained, even if barely noticeable. That effect was also expected because the hydrolysis process contributed to the water absorption increase due to partial conversion of the amide groups into carboxylic groups.

Table 3 presents the values obtained for the kinetic constants $n$ and $k$ of the studied hydrogels during swelling, as proposed by eq 1. For hydrogels in a cylindrical shape, the $n$ values between 0.45 and 0.50 correspond to Fickian diffusion. An $n$ value of approximately 1.0 indicates that the diffusion of the solvent to the interior of the gel occurs by relaxation of the chains that compose the network.[31] For $0.5 < n < 1.0$, the diffusion occurs by anomalous transport, that is, the diffusion process is carried out, simultaneously, by diffusion and relaxation of the hydrogel chains.

For the hydrogels containing calcic montmorillonite, $n$ values are between 0.5 and 1.0, indicating that the diffusion occurs by anomalous transport, while for the hydrogel without clay, the $n$ value was close to 0.5, corresponding to Fickian diffusion. For the kinetic parameter $k$, we noticed that the presence of clay in the polymeric matrix causes the hydrogel to absorb water more quickly, a factor of extreme importance for application in the agricultural sector.

**Swelling and Release.** The clay presence in the polymeric matrix of the hydrogel controlled its swelling kinetics since hydrogel 1 reaches its swelling equilibrium in approximately 10 h; while at lower concentrations, the swelling equilibrium is prolonged for 24 h. Figure 4 displays the swelling degree at equilibrium in function of the hydrogel/MMt proportion.

For the hydrolyzed hydrogels as well as for the nonhydrolyzed ones, the swelling degree was shown to be totally dependent on the ratio of the clay mineral. When the calcic montmorillonite ratio in the hydrogel polymeric matrix increases, the swelling degree reduces considerably. For the hydrogel without hydrolysis treatment, the value of the swelling degree at equilibrium ($Q_{eq}$) reduced from 90.1 ± 1.7 g/g in the hydrogel without clay to 45.8 ± 1.7 g/g in hydrogel 1. For those same hydrogels, the reduction was even more accentuated after the hydrolysis treatment. The $Q_{eq}$ values reduced from 5403.6 ± 378.9 g/g to 2188.1 ± 53.4 g/g for the hydrolyzed hydrogels 1 and 5, respectively. This can be related to the increase of the physical interlacing between the hydrogel-forming chains and the calcic montmorillonite clay lamellae. Another factor that can also contribute to the lower swelling values is the increase of the hydrogel mechanical resistance because with the more rigid chains, their expansion consequently becomes more difficult. Note that this high swelling value obtained for all the hydrolyzed sample conditions also compromises their mechanical resistance, as previously mentioned.

Table 4 displays the increase of the swelling degree caused by the hydrogel hydrolysis in water and in saturated urea solution. The considerable $Q_{eq}$ increase after hydrolysis is mostly due to the total or partial conversion of the amide groups into carboxylic groups, thus providing higher hydrogel interaction with water (see Figure 4) and also due to the swelling degree at equilibrium for the hydrogels in saturated urea solution. It is noteworthy that the pattern of variation of the swelling degree follows, for the hydrolyzed material, the same pattern observed for the nonhydrolyzed. However, in the swelling condition in the presence of urea, a reduction of 1 order of magnitude is observed in the total values, which indicates that the urea competes for the same adsorption sites as the water. Furthermore, the bidentate character of the urea can imply an increase of the intercalation of separate chains, influencing the $Q_{eq}$ decline. In this condition, the presence of the clay mineral showed inverse tendency to that observed in swelling in water, increasing the $Q_{eq}$ value according

to the increase of the clay mass in the nanocomposite. This factor is probably due to the effect of chain separation promoted by the clay mineral, which interferes in the urea adsorption avoiding the fact that its presence compacts the hydrogel structure. However, again the same sites are used.

The controlled desorption of urea test in different pHs (4, 7, and 9) was done initially with the hydrogel nanocomposites 1, 3, and 5 and with the commercial urea, i.e., without being contained in the structure of the hydrogel. The presence of the clay mineral causes the hydrogel to desorb the nutrient in a slower manner; however, it implies a reduction of the total amount of urea carried in the material due to strong clay−urea interactions. Consequently, in higher clay concentrations the hydrogel has slower desorption. This is noticed in all of the pH ranges tested, where the hydrogel without the clay mineral desorbs practically the whole nutrient in 24−48 h. However, for the nanostructured hydrogels, those values increase to approximately 72 h in the different pH values. The controlled desorption of urea curves as a function of time for the different hydrogel types at different pH values show that the urea desorption is quite responsive to pH because in the pH 4 range, as well as in 9, a higher desorption of the nutrient and lower influence of the presence of clay mineral was noted. This can be related to the counterions or electrolytes needed to promote the change in the system. Therefore, ionically charged resources could favor the release by ionic exchange or by reactions with the hydrogel structure, like hydrolysis reactions, possible in basic pH. These phenomena need to be better investigated in the future.

Figure 5 displays the kinetics of urea desorption, expressed in g of liberated urea/g of dry nanocomposite, and Table 5 displays the desorption values at the equilibrium of hydrogels at different pH values.

Besides increasing the swelling capacity, improving the dispersion of the clay in the polymer, the hydrolysis treatment significantly interferes in the controlled desorption of the urea process, increasing the amount of nutrients desorbed by the hydrogels with higher calcic montmorillonite contents in an average of 7-fold. It was also observed that desorption time increased from 72 h to values close to 200 h. From that time on, the liberation remained sustained, which is highly recommended when one seeks a hydrogel application in prolonged liberation systems. Figure 6 displays the controlled desorption of urea curves as a function of time for the different hydrolyzed hydrogels and different pH values.

Following the tendency of the hydrogels without the hydrolysis treatment, the presence of the clay mineral delayed nutrient desorption in quite a significant way. However, an important factor was that, for the hydrolyzed hydrogels, desorption time and the amount of nutrient desorbed increased significantly. Table 6 displays the values of controlled desorption of urea in different pH values for the hydrolyzed hydrogels.

The urea desorption for the hydrolyzed hydrogels was shown responsive to pH because when the pH increases from 4 to 7 and 9, the amount of the nutrient desorbed increases dramatically. A prominent factor and the most important is that the hydrolyzed hydrogels showed an inverse tendency of that which occurred in the nonhydrolyzed hydrogels; in other words, hydrogel 1 releases more nutrients than hydrogels 3 and 5. These results are not fully understood; however, it should be noted that the hydrolysis process caused the hydrogel to be better integrated into the clay mineral, which probably favored its ionic exchange effect.

The urea desorption values reached by the hydrolyzed hydrogels under study show that the hydrogels are potentially viable for agricultural application as a nutrient carrier vehicle. The total urea content for each hydrogel was also estimated, and this information was used to estimate the fractional solute release ($F_R$), considering the equilibrium of the system in water. The model developed by Reis et al.[32] was applied to fit the release from the different nanocomposite hydrogels using first and second order release kinetics. As shown in Table 7, a good accordance for the solute release in neat hydrogels for both kinetic orders was observed, by the regression $R^2$ values, where $\alpha$ values permit one to describe the solute affinity by the nanocomposite hydrogel according to the pH medium. However, for the hydrolyzed hydrogels (pure and nanocomposite), the model was only adequately fitted for first order release, which is an indicative of the easier water diffusion from nanocomposite structures to the solution. In the nanocomposites with higher hydrolyzed hydrogel contents, $F_{max}$ tended to 1, which means that the solution affinity was much higher than hydrogel affinity. This was expected since in these samples, MMt clay was shown as an effective diffusional barrier to control the urea release. Figure 7 shows an example of $F_r$ versus time for hydrogel nonhydrolyzed at pH 7.0.

In summary, it was possible to synthesize a novel nanostructured hydrogel composed of PAAm, calcic montmorillonite, and MC in different formulations. The swelling degree decreases as the clay concentration increases; however, that value increases considerably when the hydrogels undergo a hydrolysis treatment because a large part of their amide groups change to carboxylic groups. The FTIR spectra showed the presence of bands characteristic of hydrogel and clay, showing that there was an incorporation of the MMt by the hydrogel. By X-ray diffraction analyses, good nanodispersion was observed (intercalation), and exfoliation of the clay plaques in the hydrogel matrix and probably the hydrolysis of the hydrogels greatly facilitate that dispersion. The presence of clay in the hydrogels accelerated water absorption, indicated by the increase of the kinetic parameter $k$, and also increased their mechanical resistance. In a general way, the presence of the clay mineral improves some properties of the hydrogels, and the hydrogel releases the nutrient in a more prolonged manner, releasing the urea about 72 times more slowly in the hydrogel without the hydrolysis treatment and up to 192 times more slowly for the hydrolyzed hydrogels, if compared with the urea without the presence of the polymer. On the basis of such results, we highlighted the potential and viability of application of these nanocomposites containing high calcic montmorillonite content in nutrients carrier systems for the controlled release of urea. In addition, to the best of our knowledge, these nanocomposite hydrogels are the first to present this very high quantity of the urea released per hydrogel content, around 90 g per g of dry hydrolyzed hydrogel.

## ■ ASSOCIATED CONTENT

### Ⓢ Supporting Information

EDX map for the (1:1) hydrogel; FTIR spectra hydrogels; and digital photographs of the hydrogels in dry, hydrolysis, and hydrolyzed swollen states. This material is available free of charge via the Internet at http://pubs.acs.org.

## ■ AUTHOR INFORMATION

### Corresponding Author

*Embrapa Instrumentação (CNPDIA) Rua Quinze de Novembro, 1452-Sao Carlos, SP, Brazil-13560-970. Phone: +55 16 2107 2915. E-mail: caue.ribeiro@embrapa.br.

## Funding

We are grateful to Embrapa-Brazil, Fapesp, CNPq, and Capes for grants, scholarships, and financial support.

## Notes

The authors declare no competing financial interest.

## REFERENCES

(1) Ni, B.; Liu, M.; Lü, S.; Xie, L.; Wang, Y. Environmentally friendly slow release nitrogen fertilizer. *J. Agric. Food Chem.* **2011**, *59*, 10169−10175.

(2) Pereira, E. I.; Minussi, F. B.; da Cruz, C. C. T.; Bernardi, A. C. C.; Ribeiro, C. Urea montmorillonite-extruded nanocomposites: a novel slow-release material. *J. Agric. Food Chem.* **2012**, *60*, 5267−5272.

(3) Pourjavadi, A.; Barzegar, S. H.; Zeidabadi, F. Synthesis and properties of biodegradable hydrogels of κ-carrageenan grafted acrylic acid-co-2-acrylamido-2-methylpropanesulfonic acid as candidates for drug delivery systems. *React. Funct. Polym.* **2007**, *67*, 644−654.

(4) Bortolin, A.; Aouada, F. A.; Moura, M. R.; de, Ribeiro, C.; Longo, E.; Mattoso, L. H. C. Application of polysaccharide hydrogels in adsorption and controlled-extended release of fertilizers processes. *J. Appl. Polym. Sci.* **2011**, *123* (4), 2291−2298.

(5) Leone, G.; Delfini, M.; Di Cocco, M. R.; Borioni, A.; Barbucci, R. The applicability of an amidated polysaccharide hydrogel as a cartilage substitute: structural and rheological characterization. *Carbohydr. Res.* **2008**, *343*, 317−327.

(6) Zhao, L.; Xu, L.; Mitomo, H.; Yoshii, F. Synthesis of pH-sensitive PVP/CMchitosan hydrogels with improved surface property by irradiation. *Carbohydr. Polym.* **2006**, *64*, 473−480.

(7) Reddy, S. M.; Sinha, V. R.; Reddy, D. S. Novel oral colon-specific drug delivery systems for pharmacotherapy of peptide and nonpeptide drugs. *Drugs Today* **1999**, *35*, 537−580.

(8) Karada, E.; Uzum, O. B.; Saraydin, D. Water uptake in chemically crosslinked poly(acrylamide-co-crotonic acid) hydrogels. *Polym. Bull.* **2005**, *26*, 265−270.

(9) Song, F.; Zhang, L.-M.; Shi, J.-F.; Li, N.-N. Viscoelastic and fractal characteristics of a supramolecular hydrogel hybridized with clay nanoparticles. *Colloids Surf., B* **2010**, *81*, 486−491.

(10) Isiklan, N. Controlled release study of carbaryl insecticide from calcium alginate and nickel alginate hydrogel beads. *J. Appl. Polym. Sci.* **2007**, *105*, 718−725.

(11) Li, J.; Li, Y.; Dong, H. Controlled release of herbicide acetochlor from clay/carboxylmethylcellulose gel formulations. *J. Agric. Food Chem.* **2008**, *56*, 1336−1342.

(12) Haraguchi, K.; Takehisa, T.; Fan, S. Effects of clay content on the properties of nanocomposite hydrogels composed of poly(N-isopropylacrylamide) and clay. *Macromolecules* **2002**, *35*, 10162−10171.

(13) Wu, J.; Lin, J.; Zhou, M.; Wei, C. Synthesis and properties of starch-graft-polyacrylamide/clay superabsorbent composite. *Macromol. Rapid Commun.* **2000**, *21*, 1032−1034.

(14) Liu, Y.; Zhu, M.; Liu, X.; Jiang, Y. M.; Ma, Y.; Qin, Z. Y.; Kuckling, D.; Adler, H.-J.P. Mechanical properties and phase transition of high clay content clay/poly(N-isopropylacrylamide) nanocomposite hydrogel. *Macromol. Symp.* **2007**, *254*, 353−360.

(15) Zhao, Q.; Sun, J.; Lin, Y.; Zhou, Q. Study of the properties of hydrolyzed polyacrylamide hydrogels with various pore structures and rapid pH-sensitivities. *React. Funct. Polym.* **2010**, *70*, 602−609.

(16) Guo, M.; Liu, M.; Zhan, F.; Wu, L. Preparation and properties of a slow-release membrane-encapsulated urea fertilizer with superabsorbent and moisture preservation. *Ind. Eng. Chem. Res.* **2005**, *44*, 4206−4211.

(17) Xue, W.; Huglin, M. B.; Liao, B.; Jones, T. G. Swelling behaviour of crosslinked hydrogels based on (2-hydroxyethyl methacrylate) with a zwitterionic comonomer (1−3-sulfopropyl-2-vinyl-pyridinium-betaine). *Eur. Polym. J.* **2007**, *43*, 915−927.

(18) Tang, Y. F.; Du, Y. M.; Hu, X. W.; Shi, X. W.; Kennedy, J. F. Rheological characterisation of a novel thermosensitive chitosan/poly(vinyl alcohol) blend hydrogel. *Carbohydr. Polym.* **2007**, *67*, 491−499.

(19) Singh, B.; Sharma, N.; Chauhan, N. Synthesis, characterization and swelling studies of pH responsive psyllium and methacrylamide based hydrogels for the use in colon specific drug delivery. *Carbohydr. Polym.* **2007**, *69*, 631−643.

(20) Huang, L. Y.; Yang, M. C. Behaviors of controlled drug release of magnetic-gelatin hydrogel coated stainless steel for drug-eluting-stents application. *J. Magn. Magn. Mater.* **2007**, *310*, 2874−2876.

(21) Zhou, Y.; Yang, D.; Gao, X.; Chen, X.; Xu, Q.; Lu, F.; Nie, J. Semiinterpenetrating polymer network hydrogels based on water-soluble N-carboxylethyl chitosan and photopolymerized poly (2-hydroxyethyl methacrylate). *Carbohydr. Polym.* **2009**, *75*, 293−298.

(22) Yu, H.; Xiao, C. Synthesis and properties of novel hydrogels from oxidized konjac glucomannan crosslinked gelatin for in vitro drug delivery. *Carbohydr. Polym.* **2008**, *72*, 479−489.

(23) Ritger, P. L.; Peppas, N. A. A simple equation for description of solute release II: Fickian and anomalous release from swellable devices. *J. Controlled Release* **1987**, *5*, 37−42.

(24) Fu, J.; Wang, X.; Xu, L.; Meng, J..; Weng, Y.; Li, G.; He, H.; Tang, X. Preparation and in vitro−in vivo evaluation of double layer coated and matrix sustained release pellet formulations of diclofenac potassium. *Int. J. Pharm.* **2011**, *406*, 84−90.

(25) With, T. K.; Petersen, B.; Petersen, T. D. A simple spectrophotometric method for the determination of urea in blood and urine. *J. Clin. Pathol.* **1961**, *14*, 202−204.

(26) Ilavsky, M.; Hrouz, J.; Ulbrish, K. Phase transition in swollen gels. *Macromolecules* **1982**, *7*, 107−113.

(27) Jiantao, L.; Shimei, X. a.; Xiaomei, S.; Shun, F.; Jide, W. Synthesis and properties of a novel double network nanocomposite hydrogel. *Polym. Adv. Technol.* **2009**, *20*, 645−649.

(28) Yoshihiko, K.; Yoshiyuki, S.; Kazuyuki, K. Thermal transformation of a kaolinite−poly (acrylamide) intercalation compound. *J. Mater. Chem.* **1999**, *9*, 3081−3085.

(29) Spiller, K. L.; Laurencin, S. J.; Charlton, D.; Maher, S. A.; Lowman, A. M. Superporous hydrogels for cartilage repair: Evaluation of the morphological and mechanical properties. *Acta Biomater.* **2008**, *4*, 17−25.

(30) Junter, G. A.; Vinet, F. Compressive properties of yeast cell-loaded Ca-alginate hydrogel layers: Comparison with alginate−CaCO3 microparticle composite gel structures. *Chem. Eng. J.* **2009**, *145*, 514−521.

(31) Ritger, P. L.; Peppas, N. A. A simple equation for description of solute release II: Fickian and anomalous release from swellable devices. *J. Controlled Release* **1987**, *5*, 37−42.

(32) Reis, A. V.; Guilherme, M. R.; Rubira, A. F.; Muniz, E. C. Mathematical model for the prediction of the overall profile of in vitro solute release from polymer networks. *J. Colloid Interface Sci.* **2007**, *310*, 128−135.